LARGE RADIUS SELF SUPPORTING CYLINDRICAL MULTIWIRE PROPORTIONAL CHAMBERS TO BE USED AT THE ASTERIX EXPERIMENT AT LEAR*

S. AHMAD, J.C BIZOT, B. DELCOURT, J. JEANJEAN, M. JEANJEAN,

H. NGUYEN-NGOC and W.R WODRICH**

Laboratoire de l'Accélérateur Linéaire
Université de Paris-Sud, Centre d'Orsay
91405, ORSAY - France

ABSTRACT

We describe the construction and the performance of large cylindrical multiwire proportional chambers (roughly 2 meters in diameter and 1 meter long) with anode read out system. The inner and the outer cathode planes are made of foil and foam sandwiches. At 100% efficiency average anode plateau widths of about 300 volts are obtained.

* Work supported by the "Institut National de Physique Nucléaire et de Physique des Particules".

** Present address : Sektion Physik der Universitat München, 8046 Garching, FRG.

1. INTRODUCTION

The ASTERIX detector at LEAR has been designed [1,2] to study $\bar{p}p$ interactions at rest. It provides for every event simultaneous information on both the initial atomic state and the final annihilation products and can be triggered on pre-selected initial or final state configurations. A magnetic field of up to 0.8 Tesla over a cylindrical volume of 177 cm diameter and 160 cm length is provided by the solenoid of the DM1 magnetic spectrometer[3]. Antiprotons coming along the axis of the spectrometer are stopped in the H_2 gas target which is surrounded by an X-ray drift chamber (XDC) capable of detecting the X-ray atomic transitions in the 1s, 2p and 3d atomic levels of protonium. The charged particles emitted in each $\bar{p}p$ annihilation are imaged by the drift chamber and their momentum is measured by the cylindrical multiwire proportional chambers (C_1, C_2, Q_1, Q_2, P_1, Q_3 and P_2) that equip the spectrometer. Planar multiwire proportional chambers at each end cap are used to increase the solid angles for detecting gammas. A side and a front view of the experimental setup are shown in fig. 1.

Among the cylindrical chambers, the two C chambers and the three Q chambers [4] have anode and cathode detection systems and will measure the r, Φ and Z coordinates of the particle crossing points. The newly constructed large radius P chambers, with anode readout, will measure only r and Φ. Since the performances of the first constructed P_2 chamber was found not to be satisfactory, a new and more rigid P_2 chamber (P_2') was built. In this paper, the construction and the performance of these chambers P_1, P_2 (and P_2') are described.

2. DESCRIPTION OF THE CHAMBER

Our aim was to build self supporting chambers as light and as thin as possible. The chambers had to be thin as we only had 3 cm

clearance for introducing the P_2 chamber into the magnetic spectrometer. As we intend to measure the energy of charged particles, the chamber had to be light to avoid introducing unnecessary scattering in the path of the detecting charged particles. For constructing the chambers we used the technique of "foil and foam sandwich" shaped and epoxied on a rigid metallic cylindrical drum [5].

The cut away view of a typical chamber and the principal components are shown in fig. 2. For the P_1 and P_2 chambers, the inner and the outer cathode planes are made of sandwiches of graphited kapton and rohacell[§], whereas for P_2' these planes are made of sandwiches of aluminium and rohacell. The average chamber thickness in radiation length is about 3.2×10^{-3} for P_1 and about 4.5×10^{-3} and 5.0×10^{-3} for P_2 and P_2' respectively. The anode diameter is 1.4 meter for P_1 and 1.74 meter for P_2 and P_2'. The characteristics of the chambers are given in table 1.

The 20 micron gold coated rhenied tungsten anode wires having nearly 2 mm spacing were strung parallel to the chamber axis with a tension of 50 g. The total number of anode wires is 1920 for P_1 and 2698 for each of P_2 and P_2'. These wires are divided into connectors of 32 wires. The length of each anode wire is around 1 meter. The anode wires are connected to the external amplifiers by 32 wire striplines 2 to 4 meters long. We used non conducting mylar foil for the anode "guard-strips" in order to allow the operating voltage to be reduced locally by any desired amount in case of excessively noisy or broken wires by introducing a potential gradient in the defective zone.

3. PERFORMANCES

The chambers underwent a burning period using Argon-CO_2 mixtures (50% - 50%) and (80% - 20%). During the testing of the

§ Rohacell is a rigid foam of polymethacrylimide. We used rohacell 51 (50 kg/m^3)

chambers, we used the well-known magic gas mixture (Argon 80%, isobutane 19.8% and freon 0.2%). The chamber efficiency tests were made with a 1 cm^2 Sr^{90} source which provides beta rays up to 2.27 MeV. As usual the efficiencies were obtained from the coincidences between the tested chamber and a standard photomultiplier scintillation detector. For each chamber, the efficiency was measured as a function of Φ and Z co-ordinates. The over all plateau curves are shown in fig. 3. Plateau curves obtained at a number of different points through out the chamber coincide with ± 100 volts for P_1, ± 60 volts for P_2' and ± 140 volts for P_2. It is also found that the chambers can safely be operated at a maximum tension of 3.0 kv for P_1 and P_2' and 3.05 kv for P_2. At these maximum operating voltages, both P_1 and P_2' are fully efficient whereas the efficiency for a few connectors in P_2 is as low as 70%.

During our tests, we encountered some problems with P_2 concerning its shape. Initially, the uncertainties in the chamber efficiencies and plateaus as a function of Φ and Z were found to be ± 200 volts. Indeed, the variation in the total gap and gap between the anode and the cathode were found to be quite high (± 0.8 mm). The reasons were that the chambers were too sensitive to humidity. The hygroscopic constant of the rohacell and the kapton are 15×10^{-5}/% and 2×10^{-5}/% respectively and the one we measured on the sandwich after gluing was around $(7 \pm 2)\ 10^{-5}$/%. Unfortunately P_2 was built in a high humidity period, and several months later strain inside the sandwich modified the gap and thus disturbed the homogeneity.

We first tried to reshape the chamber by gluing an extra layer of 50 micron aluminium on the external surface of the chamber. The gap uncertainties found for P_2 after this modification are quoted in table 1. Another consequence of the humidity was an effect on the global current background which could also be cured by maintaining a low humidity (less than 40%) around the chamber.

Finally, we decided to rebuild another more rigid and more stable chamber P_2', by replacing the kapton on both sides of the sandwich by 50 micron aluminium foil and by adding a thicker layer of kapton as a central layer. As compared to P_2, significant improvements of the chamber characteristics were found in P_2' and we thus decided to use P_1 and P_2' at the ASTERIX experiment at LEAR[1,2].

We are grateful to Professor Perez y Jorba, Director of the LAL, for his support and encouragement. We would like to thank M. Bouessy, J. Da Costa, J. Lesueur and M. Talabardon for their help in the construction and the maintenance of the chambers.

REFERENCES

[1] S. Ahmad et al., ASTERIX Collaboration, CERN/EP 82-150.

[2] S. Ahmad et al., ASTERIX Collaboration, CERN/EP 82-165.

[3] A. Cordier et al., Nucl. Instr. and Meth. 133 (1976) 237.

[4] J. Jeanjean et al., Nucl. Instr. and Meth. 117 (1974) 349.

[5] J.E. Augustin et al., Phys. Scripta 23 (1981) 623.

TABLE 1

CHARACTERISTICS OF CHAMBERS P_1, P_2, P'_2

	P_1	P_2	P'_2
Total length of the chambers (mm)	1120	1230	1230
Internal length of the wire (mm)	960	1070	1070
Anode diameter (mm)	1400	1742	1742
Anode wire number	1920	2688	2688
Anode wire spacing (mm)	2.29	2.03	2.03
chamber thickness ($\times 10^{-3}$ radiation length)	3.2	4.5	5.0
Total gap (internal cathode to external cathode mm)	10.2 ± 0.3	10.2 ± 0.5	10.2 ± 0.2
Operating voltage (kv)	3.00	3.05	3.00
Voltage (kv) for 50% efficiency	2.73 ± 0.10	2.86 ± 0.14	2.76 ± 0.06
Mean detection efficiency at operating voltage	100%	90-100%	100%
Plateau widths for individual connectors (volts)	250 ± 50	150 ± 100	250 ± 50

FIGURE CAPTIONS

Fig. 1 . Side and front view of the ASTERIX detector

Fig. 2 . Cut away view of a typical chamber.

Fig. 3 . Current efficiency characteristics of the chambers.
(1. Global current 2. Efficiency for the best part of the chamber 3. Efficiency for the worst part of the chamber.)

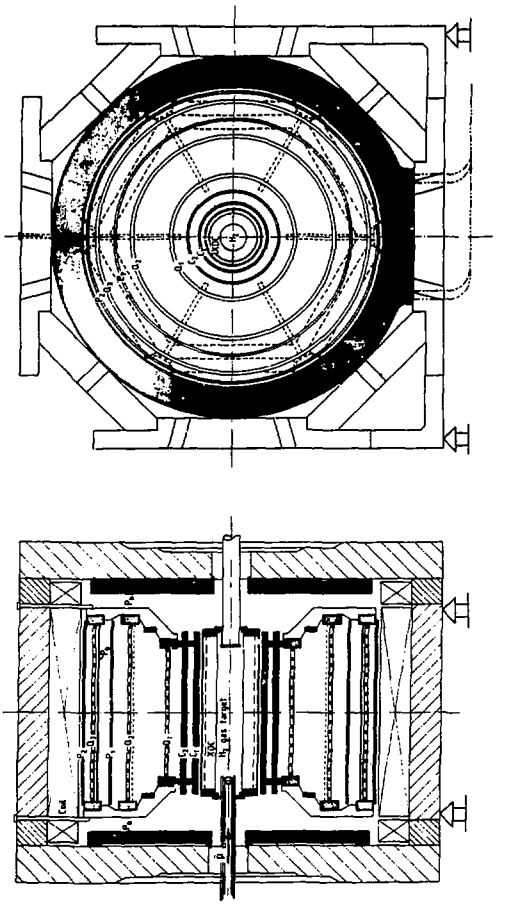

Fig. 1 . Side and front view of the ASTERIX detector

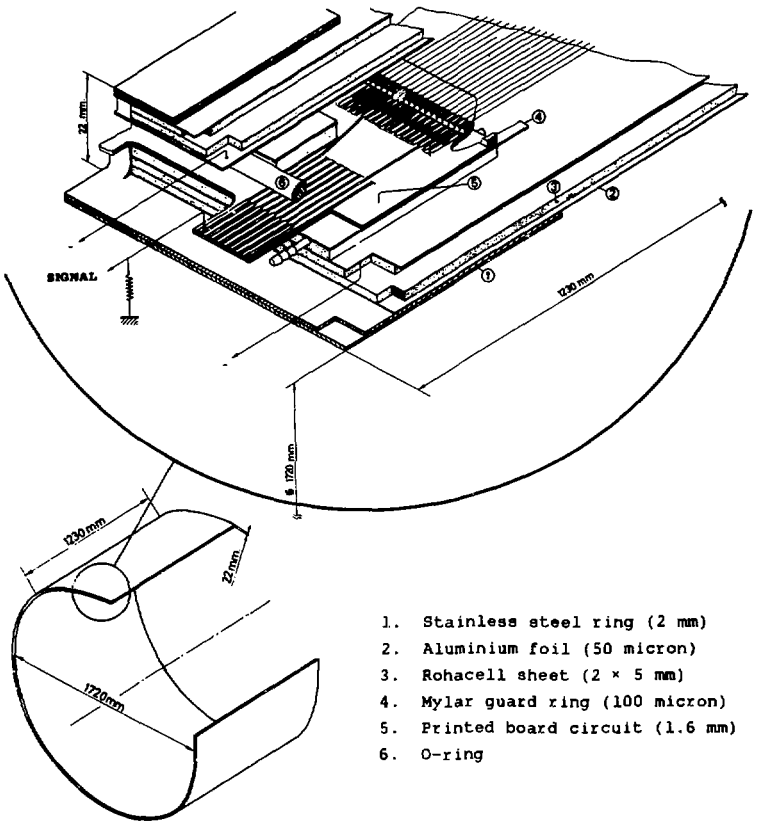

Fig. 2 . Cut away view of a typical chamber.

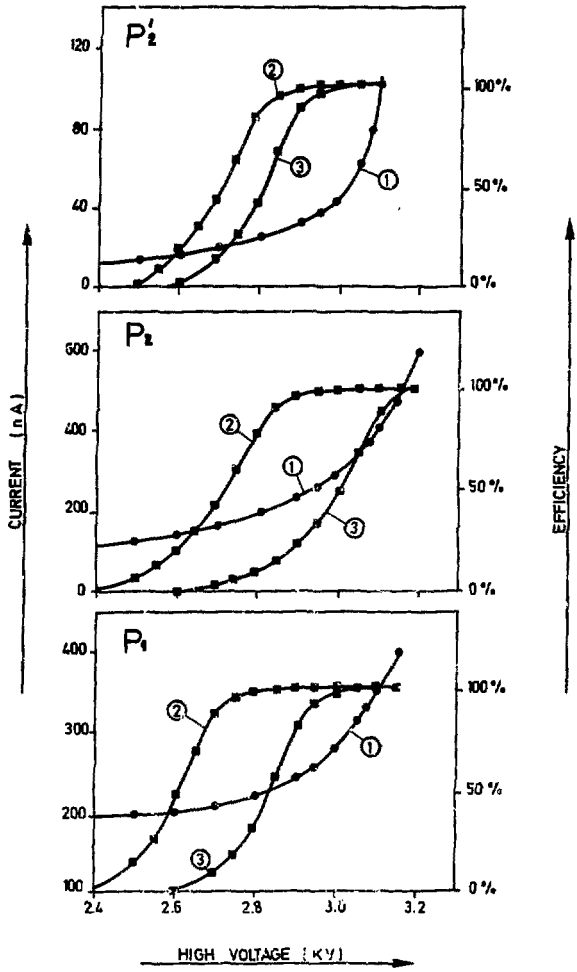

Fig. 3 . Current efficiency characteristics of the chambers.
(1. Global current 2. Efficiency for the best part of the chamber 3. Efficiency for the worst part of the chamber.)